NOTES AND CORRESPONDENCE

Inverse Determination of Surface Heat Flux over the Yellow Sea in Winter 1986 from Sea Surface Temperature Data

DONGLIANG YUAN AND Y. HSUEH

Department of Oceanography, The Florida State University, Tallahassee, Florida

30 October 1995 and 12 November 1996

ABSTRACT

An assimilation of routine sea surface temperature observations is conducted to estimate the sea surface heat flux in the Yellow Sea during the winter of 1986. Ten-day mean SST compilations, published by the Japan Meteorological Agency, are used. The time window is from 0000 Japan Local Time (JLT) 21 January to 0000 JLT 21 February 1986. Because there are only three frames of the observed temperature available for the time window, only a steady-state distribution of the heat flux is determined. A tonguelike feature of the optimized heat flux distribution is consistent with the warm SST anomaly at the center of the Yellow Sea trough. The optimized heat flux generates improved simulation of the cooling trend of the temperature time series.

The variational method is the assimilation procedure employed. The developed scheme is able to optimize simultaneously the initial temperature condition and the sea surface heat flux without a priori knowledge of either. A coarse-resolution Hessian is used to evaluate errors of the assimilation.

1. Introduction

The Yellow Sea is a shallow embayment between northern China and the Korean Peninsula. In winter, it is vertically well mixed and loses a large amount of heat to the atmosphere. Also, there are strong horizontal contrasts in temperature. A simple numerical model that incorporates wind stress and heat flux forcing has been constructed to hindcast the temperature evolution (Hsueh and Yuan 1997, hereafter referred to as HAY). The uncertainty in the specification of the sea surface heat flux is one of the primary reasons for the poor simulation of the mean cooling trend. The forward model, with its simplicity, lends itself readily to data assimilation, which provides a means for optimizing the sea surface heat flux. The procedure is further facilitated by the fact that the velocity field can be determined nearly independently of the temperature. Thus, it appears that there is the possibility that the cooling trend calculation might be improved through surface heat flux optimization. The purpose of this note is to formulate an inverse calculation of the surface heat flux through the use of data assimilation, in the vertically integrated heat equation, of regularly published sea surface temperature (SST) observations and to compare the mean cooling trend calculated from the optimized surface heat flux with that obtained in HAY.

The concept of estimating the sea surface heat flux based on the thermodynamic evolution of SST appeared in Kelly and Qiu (1995) and Yu and O'Brien (1995, hereafter referred to as YO). Kelly and Qiu, used a Kalman filter to assimilate the SST data, whereas YO used an adjoint method similar to that used in this study. However, the manner of implementation in the present study is sufficiently different from that in YO to warrant a brief report. This point can be exemplified in the following three aspects. First, YO optimize 12 frames of monthly mean heat flux and one frame of the initial temperature condition based on the mean 12-monthly SST data, making the optimization problem underdetermined because the number of data exceeds the number of unknown variables. Second, YO include additional terms in their costfunction that penalize the differences between the unknown variables and the a priori information. In contrast, the present study does not need these terms and represents a pure inverse calculation. Third, the present adjoint code is numerically consistent with the forward code, which is not assured in YO.

2. The forward model

The governing equations for the wintertime Yellow Sea circulation are contained in HAY. Based on HAY, the dynamic and thermal dynamic equations are decoupled. In addition, the open boundaries are replaced with solid walls for simplicity. In HAY, it has been shown

Corresponding author address: Prof. Ya Hsueh, Department of Oceanography, The Florida State University, Tallahassee, FL 32306-3048.
E-mail: hsueh@adin.ocean.fsu.edu

that the currents in the Yellow Sea are mostly driven by local winds; hence, closure of the open boundaries is not expected to effect a significant change in the calculated currents. Indeed, from comparisons (not shown) of current velocities to those observed at the mooring sites described in HAY there is no significant change. Also, the sea surface heat flux in the Yellow Sea and that in the East China Sea are independent of each other in this study since no coupled ocean–atmosphere model is involved. Therefore, in addressing the heat distribution in the Yellow Sea, there is little loss of realism in closing the open boundaries. The velocity fields required for calculating the advective terms in the heat equation are generated by integrating the heat and momentum equations as in HAY but with open boundaries replaced with solid walls.

The vertically integrated heat equation is finite differenced with an alternating direction semi-implicit scheme. In matrix form, the finite differencing leads to

$$\mathbf{A}_{n+1/2}\mathbf{T}_{n+1/2} = \mathbf{B}_n\mathbf{T}_n + \mathbf{f}_n,$$
$$n = 0, 1, 2, \cdots, N - 1 \tag{1}$$

for the first half–time step, and

$$\mathbf{C}_{n+1}\mathbf{T}_{n+1} = \mathbf{D}_{n+1/2}\mathbf{T}_{n+1/2} + \mathbf{g}_{n+1/2},$$
$$n = 0, 1, 2, \cdots, N - 1 \tag{2}$$

for the second half–time step.

Here $\mathbf{B}_n$, $\mathbf{A}_{n+1/2}$, $\mathbf{D}_{n+1/2}$, and $\mathbf{C}_{n+1}$ are $M \times M$ matrices that represent temperature-independent operators with coefficients at time levels indicated by the subscripts; M is the total number of computational grid points at a given time level and N is the total number of time steps of integration; $\mathbf{T}_n$ is an M-dimensional vector representing the model SST values at the computational grid points at time level n; $\mathbf{f}_n$ and $\mathbf{g}_{n+1/2}$ are M-dimensional forcing vectors at time levels n and $n + 1/2$, respectively.

The 10-day mean SST data, published by the Japan Meteorological Agency (JMA), are assimilated. Because of the small number of data frames within the 30-day time window, only the return of an average heat flux is sought from the inverse calculation in order to make the problem overdetermined. Therefore, except during the initial ramping period,

$$\mathbf{f}_n = \mathbf{g}_{n+1/2} = -2\Delta t\mathbf{Q}, \tag{3}$$

where Δt is the time step and $\mathbf{Q}$ is an M-dimensional vector representing a steady-state sea surface heat flux. The coefficient $2\Delta t$ comes from finite differencing (see Yuan 1995). The heat flux from ocean to air is defined to be positive; hence the negative sign in (3).

For numerical stability, a 6-h ramping period is used to gradually increase the sea surface heat flux from zero to its steady-state value. Thus, during the first 6 hours of the forward integration,

$$\mathbf{f}_n = -2\Delta t\frac{2n + 1}{2N_p}\mathbf{Q} \tag{3a}$$

$$\mathbf{g}_{n+1/2} = -2\Delta t\frac{2n}{2N_p}\mathbf{Q}, \tag{3b}$$

where N_p is the number of time steps within a 6-h period. The time window of data assimilation is from 0000 Japan Local Time (JLT) 21 January to 0000 JLT 21 February 1986. Thus, the total integration time of the forward model is 31 days, including the ramping period.

3. The costfunction

The costfunction in the data assimilation procedure is defined as

$$J = \sum_{i=1}^{3} 0.5(\overline{\mathbf{T}}^i - \mathring{\mathbf{T}}^i)^{\mathrm{T}}\mathbf{K}(\overline{\mathbf{T}}^i - \mathring{\mathbf{T}}^i), \tag{4}$$

where $\mathbf{K}$ is an $M \times M$ weighting matrix and $\overline{\mathbf{T}}^i$ and $\mathring{\mathbf{T}}^i$ are M-dimensional vectors representing, respectively, the model and the JMA-reported 10-day mean SST. The summation is over three time periods: 21 to 31 January, 1 to 10 February, and 11 to 20 February 1986. The model ten-day mean temperature fields are obtained by averaging 6-hourly outputs from the forward model. The independent variables in the costfunction are the initial temperature condition and the sea surface heat flux forcing and are called the control variables. The costfunction (4) does not include the control variables explicitly, nor does it contain any terms that penalize the differences between the control variables and the so-called a priori information, which is one of the fundamental differences between this study and that of YO. The convexity of the shape of the costfunction in phase space of the control variables is not obvious. Therefore, convergence of the variational procedure is not known a priori. The number of control variables is $2M$ in (4), whereas the number of temperature data is $3M$. In fact, it can be shown, both from identical-twin experiments and from a coarse-resolution Hessian calculation (see Yuan 1995), that the problem is over-determined [see Daley (1991) for the definition of an over-determined problem].

There is a statistical explanation for the construction of the costfunction (4). In order that the $\overline{\mathbf{T}}^i$ represent their maximum likelihood estimates at the minimum point of the costfunction, $\mathbf{K}$ needs to be the inverse of the error covariance matrices of the observations (Daley 1991). With the assumption that all the observational errors are random, unbiased, isotropic, homogeneous, normally distributed, and uncorrelated in space and in time, the $\mathbf{k}$ matrix here is actually an identity matrix. The model itself is assumed to be perfect. Hence the variables of the costfunction are subjected to the strong constraints of (1) and (2) (Sasaki 1970). Because the model counterparts of the observed data are all linear functions of the control variables, the least squares fit to the SST observations guarantees that the optimized

control variables represent their maximum likelihood estimates as well (Draper and Smith 1966; Thacker 1989).

The costfunction (4) is quadratic, indicating that there can be no multiple stationary points of the costfunction in phase space of the control variables. Therefore, the solution is unique provided that the problem is well posed (Gill et al. 1981).

The assimilated data are the 10-day mean SST values, published by JMA. Three frames of the 10-day mean SST fields are used to determine the model SST initial condition and the steady-state distribution of the sea surface heat flux. The JMA data are given on a 1° lat by 1° long mesh and cover all of the East China Sea and the Yellow Sea south of 38°N. To simplify the problem, a constant temperature of 3°C is assigned to the data void north of 38°N. The SST data are then interpolated onto the computational grid, using a bi-cubic spline fit. Because of the artificiality noted, the assimilation results north of 38°N are discarded.

4. The adjoint model

The objective is to minimize the costfunction (4) subject to the constraints of (1) and (2). Following Thacker and Long (1988), the M-dimensional vectors of the undetermined Lagrangian multipliers, the $\boldsymbol{\lambda}$, are introduced. Define the Lagrangian function

$$I = J + \sum_{n=0}^{N_p-1} \boldsymbol{\lambda}_{n+1/2}^{\mathrm{T}}\left(\mathbf{A}_{n+1/2}\mathbf{T}_{n+1/2} - \mathbf{B}_n\mathbf{T}_n + 2\Delta t\frac{2n+1}{2N_p}\mathbf{Q}\right) + \sum_{n=0}^{N_p-1} \boldsymbol{\lambda}_{n+1}^{\mathrm{T}}\left(\mathbf{C}_{n+1}\mathbf{T}_{n+1} - \mathbf{D}_{n+1/2}\mathbf{T}_{n+1/2} + 2\Delta t\frac{2n+2}{2N_p}\mathbf{Q}\right)$$
$$+ \sum_{n=N_p}^{N-1} \boldsymbol{\lambda}_{n+1/2}^{\mathrm{T}}(\mathbf{A}_{n+1/2}\mathbf{T}_{n+1/2} - \mathbf{B}_n\mathbf{T}_n + 2\Delta t\mathbf{Q}) + \sum_{n=N_p}^{N-1} \boldsymbol{\lambda}_{n+1}^{\mathrm{T}}(\mathbf{C}_{n+1}\mathbf{T}_{n+1} - \mathbf{D}_{n+1/2}\mathbf{T}_{n+1/2} + 2\Delta t\mathbf{Q}), \quad (5)$$

where the superscript $^{\mathrm{T}}$ represents matrix transpose.

Because (1) and (2) are satisfied, it is obvious that

$$I \equiv J. \quad (6)$$

Therefore, the minimization of the costfunction J in (6), which is a constrained optimization problem, has been transformed into the minimization of the Lagrangian function I, an unconstrained optimization problem. The stationary point of I is determined by the Euler–Lagrange equations:

$$\frac{\partial I}{\partial \boldsymbol{\lambda}_{n+1/2}} = 0, \qquad n = 0, 1, \cdots, N-1 \quad (7a)$$

$$\frac{\partial I}{\partial \boldsymbol{\lambda}_{n+1}} = 0, \qquad n = 0, 1, \cdots, N-1 \quad (7b)$$

$$\frac{\partial I}{\partial \mathbf{T}_N} = 0 \quad (7c)$$

$$\frac{\partial I}{\partial \mathbf{T}_{n+1/2}} = 0, \qquad n = 0, 1, \cdots, N-1 \quad (7d)$$

$$\frac{\partial I}{\partial \mathbf{T}_n} = 0, \qquad n = 1, 2, \cdots, N-1 \quad (7e)$$

$$\frac{\partial I}{\partial \mathbf{T}_0} = 0 \quad (7f)$$

$$\frac{\partial I}{\partial \mathbf{Q}} = 0. \quad (7g)$$

Equations (7a) and (7b) are, in fact, just (1) and (2). Equations (7c–f) are equations of the forced adjoint model. In an explicit form, they are

$$\frac{\partial I}{\partial \mathbf{T}_N} = \frac{\partial J}{\partial \mathbf{T}_N} + \mathbf{C}_N^{\mathrm{T}}\boldsymbol{\lambda}_N = 0 \quad (8a)$$

$$\frac{\partial I}{\partial \mathbf{T}_{n+1/2}} = \frac{\partial J}{\partial \mathbf{T}_{n+1/2}} + \mathbf{A}_{n+1/2}^{\mathrm{T}}\boldsymbol{\lambda}_{n+1/2} - \mathbf{D}_{n+1/2}^{\mathrm{T}}\boldsymbol{\lambda}_{n+1} = 0 \quad (8b)$$

$$\frac{\partial I}{\partial \mathbf{T}_n} = \frac{\partial J}{\partial \mathbf{T}_n} + \mathbf{C}_n^{\mathrm{T}}\boldsymbol{\lambda}_n - \mathbf{B}_n^{\mathrm{T}}\boldsymbol{\lambda}_{n+1/2} = 0 \quad (8c)$$

$$\frac{\partial I}{\partial \mathbf{T}_0} = \frac{\partial J}{\partial \mathbf{T}_0} - \mathbf{B}_0^{\mathrm{T}}\boldsymbol{\lambda}_{1/2} = 0. \quad (8d)$$

Equation (7g) yields

$$\frac{\partial I}{\partial \mathbf{Q}} = 2\Delta t \sum_{n=0}^{N_p-1}\left(\frac{2n+1}{2N_p}\boldsymbol{\lambda}_{n+1/2} + \frac{2n+2}{2N_p}\boldsymbol{\lambda}_{n+1}\right) + 2\Delta t \sum_{n=N_p}^{N-1}(\boldsymbol{\lambda}_{n+1/2} + \boldsymbol{\lambda}_{n+1}) = 0. \quad (9)$$

Usually, (8a–d) and (9) cannot be solved directly for the initial condition and the sea surface heat flux. An iteration strategy is used in the variational procedure to approach the solution sequentially. First, the forward model with a ''guess'' SST initial condition and sea surface heat flux, is integrated forward to produce the model-minus-data misfit fields so that ($\partial J/\partial \mathbf{T}_{n+1/2}$, $\partial J/\partial \mathbf{T}_n$) in (8a–d) are known. Then, the forced adjoint model (8a–c) is integrated backward in time to yield the gradients of the Lagrangian function with respect to the initial condition and the sea surface heat-flux fields; namely,

$$\frac{\partial I}{\partial \mathbf{T}_0} = \frac{\partial J}{\partial \mathbf{T}_0} - \mathbf{B}_0^{\mathrm{T}} \boldsymbol{\lambda}_{1/2} \tag{10a}$$

$$\frac{\partial I}{\partial \mathbf{Q}} = 2\Delta t \sum_{n=0}^{N_p-1} \left(\frac{2n+1}{2N_p} \boldsymbol{\lambda}_{n+1/2} + \frac{2n+2}{2N_p} \boldsymbol{\lambda}_{n+1} \right) + 2\Delta t \sum_{n=N_p}^{N-1} (\boldsymbol{\lambda}_{n+1/2} + \boldsymbol{\lambda}_{n+1}). \tag{10b}$$

If the guess SST initial condition and sea surface heat flux are not the optimal solution, (7f) and (7g) are not satisfied. Once the gradient in (10a,b) is known, certain descent algorithms [e.g., the LBFGS subroutine (Zen et al. 1993)] can be employed to adjust the guess SST initial condition and sea surface heat flux fields. The forward model is then integrated again with the corrected SST initial condition and sea surface heat flux to update the data misfit fields. The iteration continues until the norm of the gradient (10a,b) is less than a small number. (The norm of a vector in this study is defined to be the inner product of the vector with itself.) By that time, the SST initial condition and the sea surface heat flux are considered optimized, because (7a–g) are all satisfied, and the least squares fit is accomplished. The descent algorithm used is the limited-memory quasi-Newton method of Liu and Nocedal (1989).

After the numerical codes for (8a–d) are constructed, it is very important to examine whether the codes yield the correct gradient information. Here use is made of the test suggested by Navon et al. (1992). Suppose $\mathbf{Y}$ is a $2M$ dimensional random vector; it follows that

$$\varphi(\theta) = \frac{J(\mathbf{X} + \theta\mathbf{Y}) - J(\mathbf{X})}{\theta \mathbf{Y}^{\mathrm{T}} \cdot \nabla J(\mathbf{X})} = 1 + o(\theta). \tag{11}$$

Here

$$\mathbf{X} = \begin{pmatrix} \mathbf{T}_0 \\ \mathbf{Q} \end{pmatrix}$$

represents the $2M$-dimensional control variable vector,

$$\nabla J(\mathbf{X}) = \begin{pmatrix} \dfrac{\partial J}{\partial \mathbf{T}_0} \\ \dfrac{\partial J}{\partial \mathbf{Q}} \end{pmatrix}$$

is the $2M$-dimensional gradient vector, and θ is a small scalar parameter.

For values of θ that are small, but not too close to the machine zero, one should expect $\varphi(\theta)$ to be close to 1. Equation (11) represents a very strict test because both the numerator and the denominator must go to zero at exactly the same rate. The numerator is calculated by the forward model integration, whereas the gradient of the costfunction in the denominator is obtained through integration of the forced adjoint model. Figure 1 shows the variations of φ with θ for the present calculation. For values of θ less than 10^{-5} and larger than 10^{-12}, the value of φ is very close to 1.0, suggesting numerical consistency between the forward and adjoint models. A similar consistency test was not shown in the YO paper, probably because they derive the adjoint equation analytically from the heat equation and then finite difference the adjoint equation independent of the forward model scheme. An indication of pitfalls in their treatment is that they report the existence of multiple stationary points of the costfunction, which should not exist. The importance of numerical consistency in the variational procedure has been reported in the literature (see, e.g., Zou and Navon 1993).

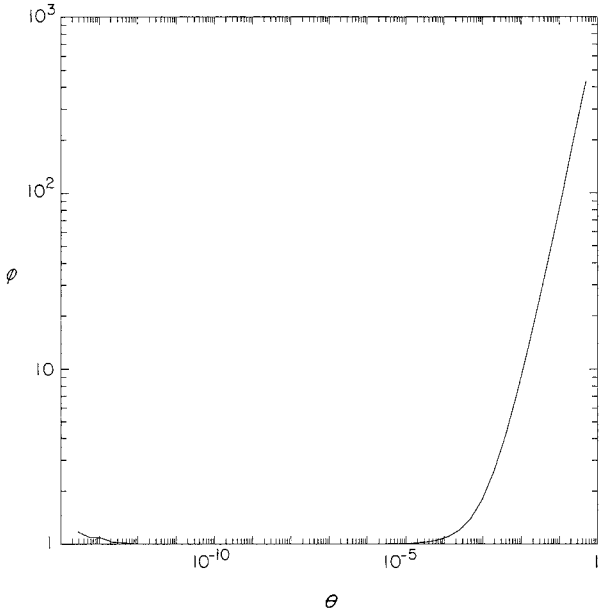

FIG. 1. Plot of $\varphi(\theta)$ in (11) showing consistency of the forward and adjoint model pair.

5. Results from using real SST data

The inverse calculation of both the temperature initial condition and surface heat flux from the 10-day mean SST compilations of the JMA will now be discussed. The assimilation is conducted in double precision, and the results are shown in Figs. 2–4.

Figures 2a and 2b show the variation of the costfunction and of the norm of the gradient with iteration steps. At the end of the optimization, the costfunction is reduced by one order of magnitude and the norm of the gradient has decreased more than three orders of magnitude. The consistent decrease of both the costfunction and the norm of the gradient indicates that the inverse calculation is successful.

Also examined are the optimized temperature initial condition and sea surface heat flux (Figs. 2c,d). The optimized initial condition has a similar spatial structure as that of the 10-day mean SST data. Because of the optimization of the initial temperature condition, the

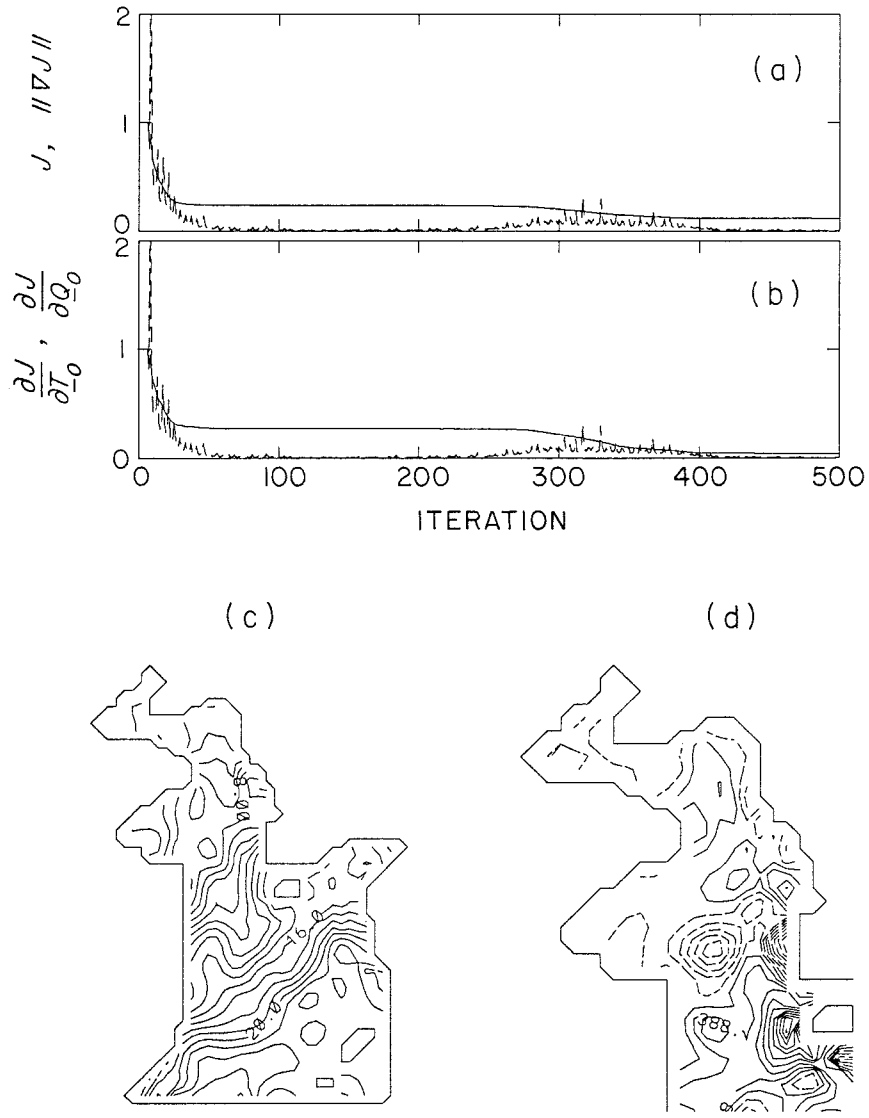

FIG. 2. Results from using the JMA 10-day mean SST data: (a) costfunction (solid) and norm of its gradient (dash) vs iteration steps; (b) norms of the gradient of the costfunction with respect to initial condition (solid) and with respect to sea surface heat flux (dash). In (a) and (b) the curves have been normalized by their values at the fifth iteration. (c) Optimized initial condition, ranging from 3°C to 24°C, contoured at intervals of 1°C. (d) Optimized sea surface heat flux, ranging from -1.6×10^3 to 2.0×10^3 cal cm^{-2} day^{-1}, contoured at intervals of 2×10^2 cal cm^{-2} day^{-1}. Negative values are drawn with dash contours. The first solid contour represents the value of 88.0 cal cm^{-2} day^{-1}.

simulated temperatures are closer to the observed temperatures than in HAY in absolute values. The inversely calculated sea surface heat flux in the Yellow Sea reveals a rich spatial structure. Starting from a region of large heat loss west of Cheju Island, there is a ''tongue'' of upward sea surface heat flux extending into the northern reaches of the Yellow Sea along the central trough. This tonguelike structure is thought to be associated with the northward intrusion of Kuroshio water and is consistent with the observed SST warm tongue structure (see HAY). At the northern tip of the structure in the center of the Yellow Sea, the tongue is flanked by two centers of negative heat flux, one to the west and the other to the east. Farther to the north, two centers of weakly upward heat flux are produced by the calculation. A local maximum of heat loss is produced off the China coast at about the same latitude as Cheju. The distribution of the steady-state sea surface heat flux seems to have a north–south structure of high–low–high values along both flanks of the Yellow Sea trough. The existence of this structure is yet to be explained.

With the optimized initial condition and steady-state

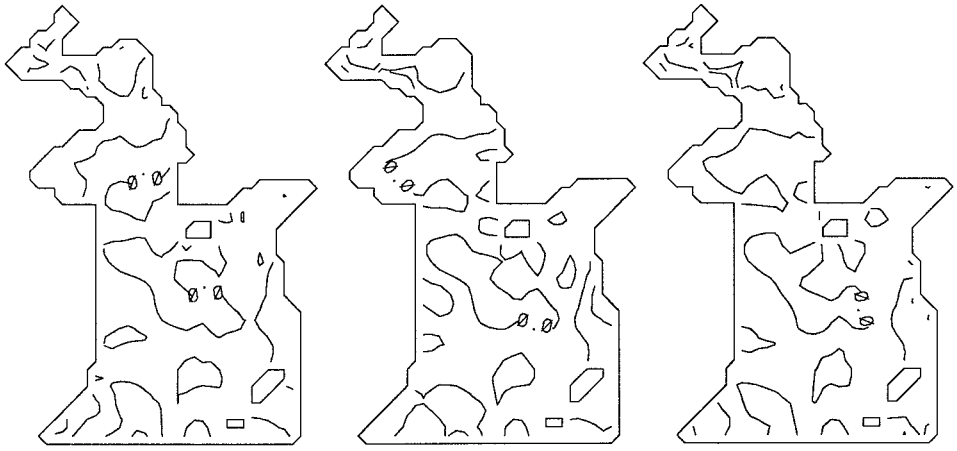

FIG. 3. Data misfit fields after the optimization for (a) 21–31 January, (b) 1–10 February, and (c) 11–20 February. Contour intervals are 1°C. The magnitudes of the misfit are around ±1°C.

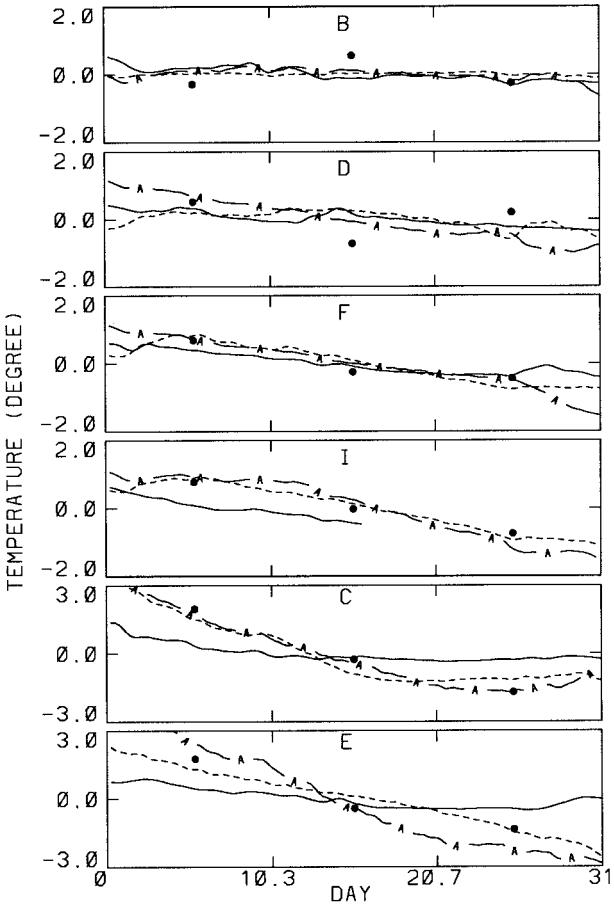

FIG. 4. Comparisons of demeaned temperature time series at the six mooring stations described in HAY. Solid curves are from the moorings, short-dashed are the optimized model simulations, and long-dashed with the A's are from HAY where no assimilation was involved. The solid circles represent the JMA 10-day mean SST data. In panels C and E, the coordinate scale is 3°C, whereas in panels B, D, F, and I, the scale is 2°C.

sea surface heat flux (Figs. 2c and 2d), the forward model generates a set of model solutions. A characteristic of all these model-minus-data misfit fields is that the misfits display random spatial distributions, which confirms that the model represents the correct dynamic link between the frames of the 10-day mean SST compilations and that the assimilation scheme has extracted the maximum amount of dynamical information from the data.

The optimized cooling trends at the mooring stations are compared with in situ observations in (Fig. 4). None of the moored observations have been used by the minimization procedure, and the consistency of the 10-day mean SST compilations with the moored observations is subject to observational errors. All of the simulated cooling trends except at station B are closer to the observed trends than in HAY (see Table 1). (At station B, the HAY simulation, was already very good; thus, the assimilation could not make further improvement because neither the JMA data nor the model are perfect.) The optimized cooling trends at mooring stations C and E still have large discrepancies compared with the in situ observations. However, one can easily identify, from the SST data (see the circles in Fig. 4), that the optimization procedure has done its best to reduce the errors of the least squares fit. The remaining discrepancies are apparently due to biases in the 10-day mean SST compilations.

An uncertainty analysis of the optimization has been carried out on the basis of a coarse-resolution Hessian matrix (Yuan 1995). It is found that the uncertainties amount to about ±1°C in the initial temperature condition and 381 W m^{-2} in sea surface heat flux at the 90% confidence level. Thus, both the two negative (air-to-ocean) sea surface heat flux centers straddling the Yellow Sea trough and the positive (ocean-to-air) sea surface heat flux center west of Cheju are statistically significant. The relative position of the three centers frames well the

TABLE 1. Comparison of the linear regression slopes at the mooring stations (unit in 0.01°C/day).

	B	D	F	I	C	E
Mooring	−1.92	−2.17	−3.21	−6.17	−3.60	−4.09
Assimilation	−0.08	−1.74	−5.78	−7.15	−14.0	−14.0
HAY	−0.9	−6.76	−7.44	−9.42	−16.0	−24.0

tongue of positive sea surface heat flux that extends from west of Cheju into the Yellow Sea along the trough.

The error covariance estimate from the Hessian calculation is an underestimate of the full error covariances, because no account has been made of the errors in the heat advection simulation. The two negative centers in the central Yellow Sea are counterintuitive because in winter the Yellow Sea should lose heat to the atmosphere above. These errors are probably caused by the errors in the heat advection simulation. (In HAY, it has been shown that the simulated velocity in the nearshore region is still far from the observations.) An inspection (not shown) of the balance of the terms of the heat equation inside the negative centers indeed indicates that the temporal change of temperature and the heat flux terms are both negative and are balanced by the positive heat advection. This result suggests that further improvement of the temperature simulation in the nearshore region has to rely primarily on an improvement of the velocity simulation near the coast.

6. Discussion and conclusions

An example of inversely calculating the sea surface heat flux from routinely compiled SST data has been presented. The variational procedure used is distinguished from a previous study in that it can successfully handle an overdetermined problem. The construction of the costfunction does not require any a priori information about the control variables. A numerical consistency test is conducted to verify the correctness of the adjoint code.

A mean sea surface heat flux over the Yellow Sea in 1986 winter for the period of 21 January–20 February is determined from assimilating the 10-day mean SST compilations published by JMA. The calculated sea surface heat flux is rich in spatial structure with a tongue of upward flux extending from west of Cheju Island into the northern reaches of the Yellow Sea, consistent with the existence of the warm tongue along the center of the Yellow Sea trough. On both flanks of the Yellow Sea trough, the sea surface heat flux has a north–south spatial distribution of high–low–high values. The reason for this structure is not yet known. The existence of two negative centers of the sea surface heat flux on both flanks of the Yellow Sea trough is counterintuitive, and they are probably caused by errors in the heat advection simulation off the center of the Yellow Sea trough. All cooling trends at the mooring stations except at station B are closer to those in the in situ observations after the assimilation.

The results of an uncertainty analysis, based on a coarse-resolution Hessian calculation, suggests that the spatial structure of the sea surface heat flux resolved by the inverse calculation is statistically significant.

Acknowledgments. This research is supported by the National Science Foundation Grants OCE-9115365 and OCE95-29289, by the Coastal Sciences Program of the Office of Naval Research Grant N00014-90-J-1820, by the Physical Oceanography Program of the Office of Naval Research Grant N00014-95-1-0501, and by the Minerals Management Service Cooperative Agreement 14-35-0001-30804. The first author wishes to express his gratitude to Mr. Takashi Yoshida of the Oceanographical Division of the Japan Meteorological Agency for providing the 10-day mean sea surface temperature data.

REFERENCES

Daley, R., 1991: *Atmospheric Data Analysis.* Cambridge University Press, 457 pp.

Draper, N. R., and H. Smith, 1966: *Applied Regression Analysis.* John Wiley, 407 pp.

Gill, P. E., W. Murray, and M. H. Wright, 1981: *Practical Optimization.* Academic Press, 401 pp.

Hsueh, Y., and D. Yuan, 1997: A numerical study of currents, heat advection and sea-level fluctuations in the Yellow Sea in winter of 1986. *J. Phys. Oceanogr.,* **27,** 2313–2326.

Kelly, K. A., and B. Qiu, 1995: Heat flux estimates for the western North Atlantic. Part I: Assimilation of satellite data into a mixed layer model. *J. Phys. Oceanogr.,* **25,** 2344–2373.

Liu, D. C., and J. Nocedal, 1989: On the limited memory BFGS method for large scale minimization. *Math. Prog.,* **45,** 503–528.

Navon, I. M., X. Zou, J. Derber, and J. Sela, 1992: Variational data assimilation with an adiabatic version of the NMC spectral model. *Mon. Wea. Rev.,* **120,** 1433–1446.

Sasaki, Y., 1970: Some formations in numerical variational analysis. *Mon. Wea. Rev.,* **98,** 875–883.

Thacker, W. C., 1989: The role of the Hessian matrix in fitting models to measurements. *J. Geophys. Res.,* **94,** 6177–6199.

——, and R. B. Long, 1988: Fitting dynamics to data. *J. Geophys. Res.,* **93**(C2), 1227–1240.

Yu, L., and J. J. O'Brien, 1995: Variational data assimilation for determining the seasonal net surface heat flux using a tropical Pacific model. *J. Phys. Oceanogr.,* **25,** 2319–2343.

Yuan, D., 1995: Toward the prediction of surface temperature in the Yellow Sea in winter. Ph.D. dissertation, The Florida State University, 177 pp. [Available from DIRAC Library, The Florida State University, Tallahassee, FL 32306.]

Zou, X., and I. M. Navon, 1994: Variational data assimilation: Some aspects of theory and application. *Environmental Modeling,* Vol. II, *Computer Methods and Software for Simulating Environmental Pollution and Its Adverse Effects,* P. Zannetti, Ed., Failure Analysis Associates Inc., 277–325.

——, ——, M. Berger, M. K. Phua, T. Schlick, and F. X. LeDimet, 1993: Numerical experience with limited-memory, quasi-Newton methods for large-scale unconstrained nonlinear minimization. *SIAM J. Optimization,* **3,** 582–608.